Journal Name

ARTICLE TYPE

Cite this: DOI: 10.1039/xxxxxxxxxx

Supplementary information for Packing and Dynamics of a Protein Solution Approaching the Jammed State

Nafisa Begam,[a*] Stefano Da Vela,[a,1] Olga Matsarskaia,[a,2] Michal K. Braun,[a] Alessandro Mariani,[b,3] Fajun Zhang,[a*] and Frank Schreiber [a]

Received Date
Accepted Date

DOI: 10.1039/xxxxxxxxxx

www.rsc.org/journalname

1 Determination of structure factors from SAXS profiles

In order to determine the structure factor, S(q), we have used a SAXS profile collected on a dilute BSA solution (5 mg/ml) as the form factor, P(q) and calculated $S(q)$ via the relation

$$S(q) \approx I(q)/P(q) \quad (1)$$

where $I(q)$ is the intensity profile collected during the SAXS measurement. Figure S1 shows the $P(q)$ used for the current analysis according to eqn. 1.

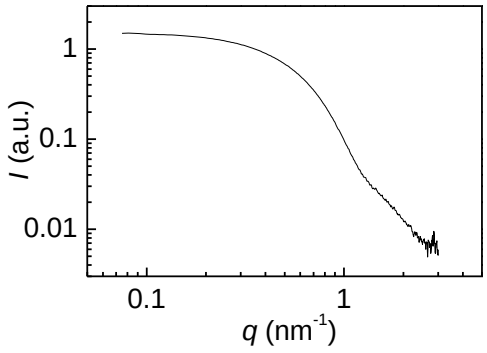

Fig. S1 SAXS intensity profile of a dilute (5 mg/ml) BSA solution corresponding to the form factor, $P(q)$, of BSA. This $P(q)$ was used to determine $S(q)$ from the measured $I(q)$.

From the $S(q)$ thus obtained, we estimated q_{max} by fitting only the peaks of $S(q)$ with a single peak Gaussian function given by

$$y = y_0 + A * e^{-(q-q_{max})^2/\omega^2} \quad (2)$$

where ω is the width of the peak, y_0 and A are fit parameters. Several typical fits at different evaporation times are shown in Fig. S2.

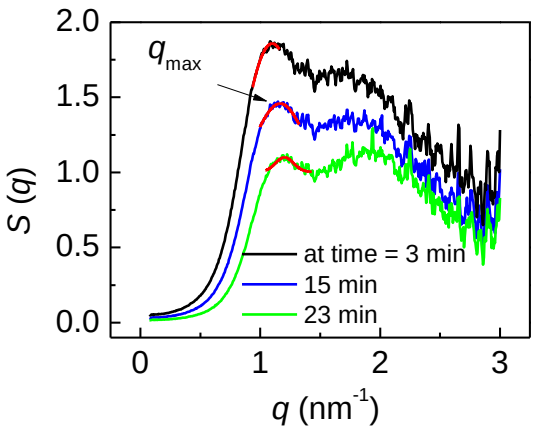

Fig. S2 Typical single peak Gaussian fits (eqn. 2) clearly showing the position of the peaks of $S(q)$ providing q_{max} at different evaporation times as indicated in the figure.

2 pH of the aqueous BSA solution

We measured the pH value of the individual BSA solutions which are used for the calibration of c_p dependence ξ (for c_p = 27-301 mg/ml) in the current study. The pH values of the solution as a

[a] Institut für Angewandte Physik, Universitat Tübingen, 70276, Tübingen, Germany, E-mail: nafisa.begam@uni-tuebingen.de, fajun.zhang@uni-tuebingen.de
[b] ESRF-The European Synchrotron, 71 Avenue des Martyrs, 38000, Grenoble, France
[1] Present affiliation: EMBL c/o DESY, Notkestr. 85, 22607 Hamburg, Germany
[2] Present affiliation: Institut Laue-Langevin, 71 Avenue des Martyrs, 38042 Grenoble, France
[3] Present affiliation: Helmholtz-Institut Ulm für elektrochemische Energiespeicherung, Helmholtzstr. 11, 89081 Ulm, Germany

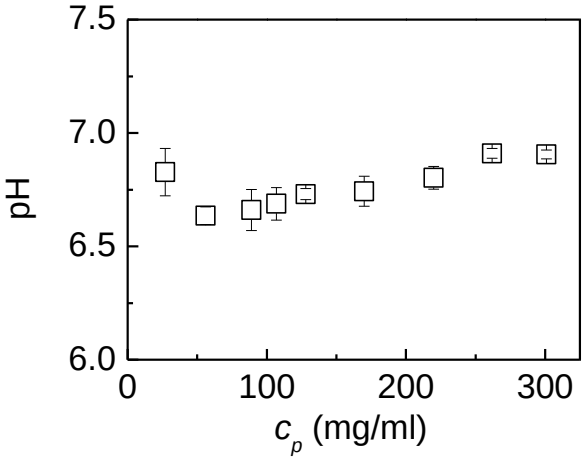

Fig. S3 pH values of BSA solutions with different c_p, showing an almost constant pH value of 6.8 $\pm$ 0.2 throughout the entire concentration range.

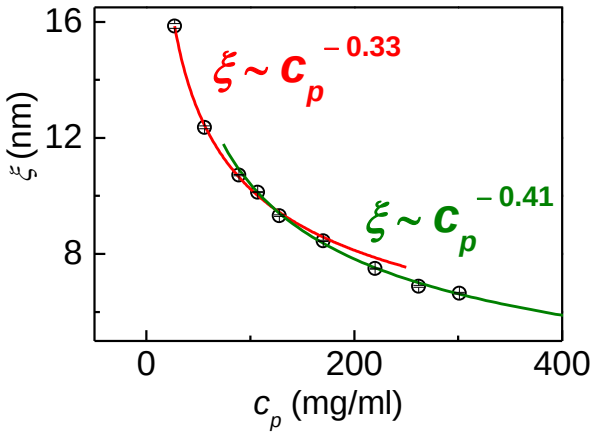

Fig. S5 ξ as a function of c_p obtained from SAXS measurements ($S(q)$) on a linear scale showing a clear change in the power law dependence of ξ on c_p.

function of c_p (Fig. S3) show a constant pH value of 6.8 $\pm$ 0.2 throughout the entire c_p range.

3 Power law relation of ξ and c_p

The power law dependence of the characteristic length scale ξ as a function of c_p with an exponent of 0.33 has been successfully shown by several studies [1,2]. However, the current study seems to indicate a deviation from this conventional value mainly due to the ellipsoidal shape of BSA and its deformation at high packing density [3]. Most likely, these effects influence the exponent at high concentrations when the particles start touching each other.

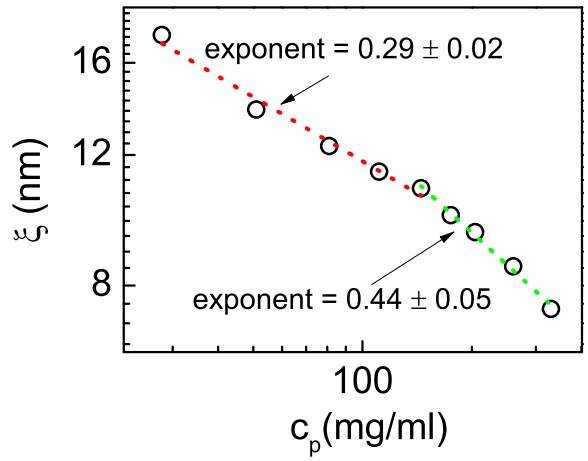

Fig. S4 ξ vs c_p collected using a laboratory X-ray source reproducing the change in the power law exponent at high c_p which is also seen in Fig. S4.

We have reproduced the relation between ξ vs c_p using a laboratory X-ray source (Fig. S4). In this case, the ξ values are extracted from the $I(q)$ profiles.

The change in the exponent (shown in Fig. 2 of the main manuscript) can be visualized clearly when ξ vs c_p is plotted on a linear scale in Fig. S5.

4 Single power law fit

For comparison, we have modeled the full range of data (Fig. 2 in the main manuscript) with a single power law and obtained an exponent of 0.36 (Fig. S6). Using this value we have recalculated the concentrations and corresponding volume fractions which are shown in Fig. S7.

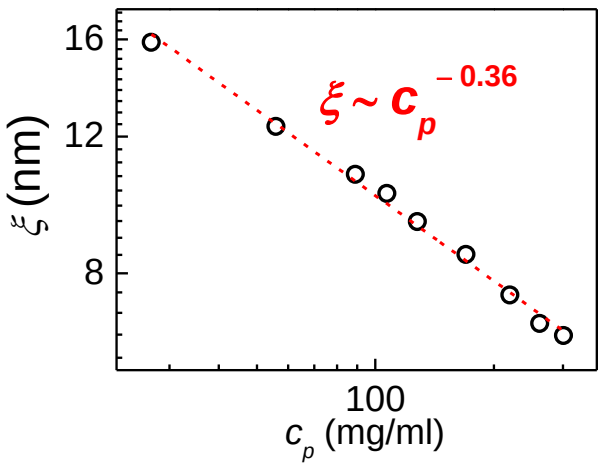

Fig. S6 ξ vs c_p modelled with a single power law with an exponent of 0.36 over the entire range of c_p measured.

Since the starting point of regime (2) (at ξ = 6.8 nm) is not influenced by the calculation procedure, Fig. S7 shows that the system is in regime (2) in the beginning of the drying measurements and then enters the jammed state at $\phi \approx 0.47$ (as indicated

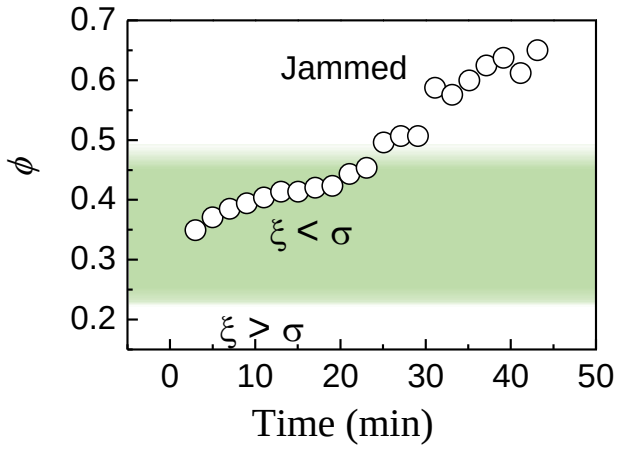

Fig. S7 ϕ estimated from the single power law dependence of ξ on c_p (Fig. S6) as a function of drying time.

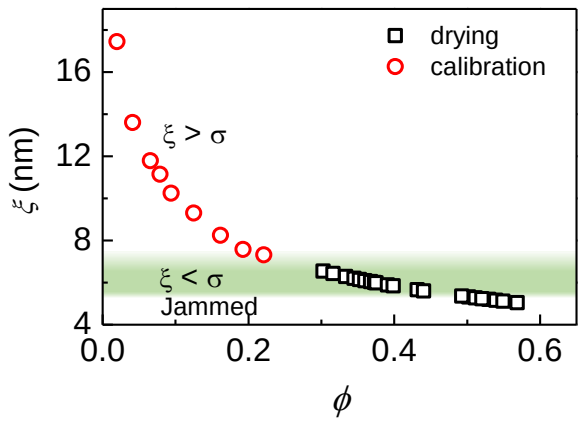

Fig. S9 Center-to-center particle distance estimated using the relation $\xi = 2.25\pi/q_{max}$ from the individual solutions (red circles) (for the calibration of ξ vs c_p) and during drying (black squares) as a function of ϕ.

in Ref. 4). As can be seen here, the overall behavior of the presence of three regimes (using single power law) remains the same as that obtained by two power law fit to ξ vs c_p.

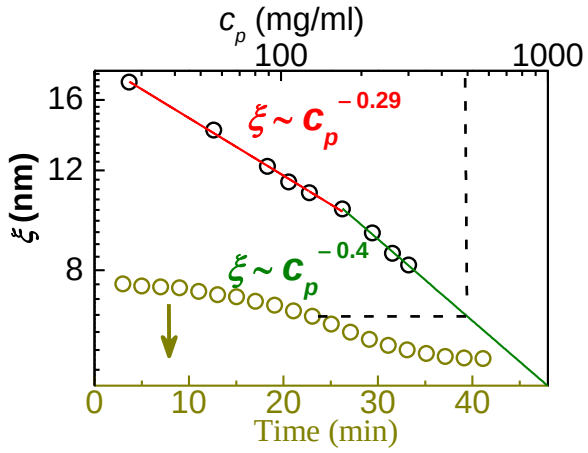

Fig. S8 ξ as a function of c_p (top x-axis) estimated from SAXS intensity profiles $I(q)$ for individual solutions (black circles) exhibits a power law, $\xi \sim c_p^{\alpha}$, with α = 0.29 (red line) and α = 0.4 (green line) for c_p below and above 200 mg/ml, respectively, and during drying (dark yellow circles) as a function of drying time (bottom x-axis).

Figure S8 shows ξ estimated from SAXS intensity profiles in the calibration regime (black circle) and during the drying (dark yellow circles).

5 Packing volume fraction calculated based on new model

In order to compare the drying behavior of proteins to the spherical colloidal model where the center-to-center pair distance is taken as $\xi = 2.25\pi/q_{max}$ [5,6], we have recalculated the ξ values (previously calculated as $\xi = 2\pi/q_{max}$). Note that this relation does not influence the values of the estimated concentrations and volume fractions during drying. The newly estimated ξ as a function of ϕ is shown in figure S9. Similar to the results shown in Fig. 3, the result here shows that the solution is in regime (1) in the calibration regime, enters into regime (2) in the beginning of drying (at $\phi \sim 0.3$) and eventually reaches a jammed state at $\phi \approx 0.47$.

6 Comparison with the dimensions of the BSA crystal structure

For analysis, in this report, the hydrodynamic diameter of BSA (= 6.8 nm) [7] was taken as the protein diameter to compare the length scale, ξ, obtained from the SAXS measurements. However, if we compare ξ with the dimension of BSA (hydrated) obtained from its crystal structure (PDB 3V03 [8]) which is 1.7 x 4.2 x 4.2 nm^3, we can see that the length scale observed here does not reach values smaller than 2×1.7 nm (the minor axis of the ellipsoid) at the highest volume fraction measured. Therefore, it is possible that the ellipsoidal protein molecules are not deformed but only aligned leading to a much smaller inter-protein distance than the major axis dimension of the ellipsoid. However, in this case the correlation peak would be expected to be visible until the end of the drying process.

7 Calculation of BSA volume

In the current report, we have used the molecular volume of BSA estimated using the method described below.

The mass of one protein monomer is approximately equal to its molecular weight divided by the Avogadro number

$= 66.5 \times 10^3/6.023 \times 10^{23} = 1.104 \times 10^{-19}$ g

Therefore, the volume of one monomer is equal to the product of monomer mass and its specific volume

$= 1.104 \times 10^{-19} \times 0.735 = 81 \times 10^{-21}$ cm^3

$= 81$ nm^3

This value is very close to the value (~ 88.2 nm^3) reported in Ref. 4.

8 Calculation of volume fraction from mass fraction

In order to compare the currently observed BSA volume fraction range with the reported critical mass fraction of BSA in Ref. 4, we converted the critical mass fraction into corresponding volume fraction.

The mass fraction of 0.55 corresponds to the volume fraction,
ϕ = (volume of proteins)/(volume of proteins + volume of solvent)
$= \frac{0.55\times0.735}{(0.55\times0.735)+0.45}$
$= 0.47$
Similarly a mass fraction of 0.6 corresponds to $\phi = 0.52$.

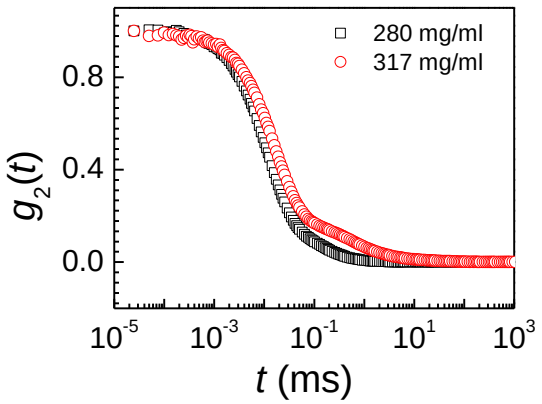

Fig. S10 $g_2(t)$ at two c_p values as indicated in the legends.

9 Dynamics: Single to two-step relaxation decay

We compared $g_2(t)$ collected on solutions with c_p of 280 and 317 mg/ml in Fig. S10.

We can see here that the secondary relaxation for the solution with c_p = 280 mg/ml is minor while that for the solution with c_p = 317 mg/ml is pronounced. This suggests that the transition from a single to a two-step exponential decay occurs between 280 mg/ml and 317 mg/ml (i.e. between $\phi \sim$ 0.21-0.23)

Notes and references

1 G. M. Conley, P. Aebischer, S. Nöjd, P. Schurtenberger and F. Scheffold, *Sci. Adv.*, 2017, **3**, e1700969.

2 A. Stradner, H. Sedgwick, F. Cardinaux, W. C. Poon, S. U. Egelhaaf and P. Schurtenberger, *Nature*, 2004, **432**, 492.

3 A. Donev, I. Cisse, D. Sachs, E. A. Variano, F. H. Stillinger, R. Connelly, S. Torquato and P. M. Chaikin, *Science*, 2004, **303**, 990–993.

4 G. J. Brownsey, T. R. Noel, R. Parker and S. G. Ring, *Biophys. J.*, 2003, **85**, 3943–3950.

5 M. L. de Haro and M. Robles, *J. Phys. Cond. Matt.*, 2004, **16**, S2089.

6 J. Liu, H.-J. Schöpe and T. Palberg, *Part. Part. Syst. Charact.*, 2000, **17**, 206–212.

7 F. L. González Flecha and V. Levi, *Biochem. Mol. Biol. Edu.*, 2003, **31**, 319–322.

8 K. A. Majorek, P. J. Porebski, A. Dayal, M. D. Zimmerman, K. Jablonska, A. J. Stewart, M. Chruszcz and W. Minor, *Molecular Immunology*, 2012, **52**, 174–182.